ACS OMEGA

Open Access

http://pubs.acs.org/journal/acsodf

Article

Agarperoxinols A and B: Two Unprecedented Tricyclic 6/6/7 Rearranged Humulene-Type Sesquiterpenoids That Attenuated the Neuroinflammation in LPS-Stimulated Microglial Models

Chi Thanh Ma, Sang Bin Lee, In Ho Cho, Jae Sik Yu, Tianqi Huang, Tae Min Lee, Tu Loan Ly, Sung Won Kwon, Jeong Hill Park, and Hyun Ok Yang*

Cite This: *ACS Omega* 2023, 8, 43873−43882

Read Online

ACCESS | Metrics & More | Article Recommendations | Supporting Information

ABSTRACT: Agarperoxinols A and B (**1**−**2**), two naturally occurring humulene-type sesquiterpenoids with an unprecedented tricyclic 6/6/7 ring, were discovered from the agarwood of *Aquilaria malaccensis*. Their structures were unambiguously determined by various spectroscopic data, experimental ECD calculations, and single-crystal X-ray diffraction analysis. Agarperoxinol B showed significant and dose-dependent neuroinflammatory inhibitory effects on various proinflammatory mediators, including NO, TNF-α, IL-6, and IL-1β, and suppressed iNOS and COX-2 enzymes in LPS-activated microglial cells. A mechanistic study demonstrated that agarperoxinol B remarkably inhibited the phosphorylation of the Akt and JNK signaling pathways. Agarperoxinol B also significantly reduced the expression of the microglial markers Iba-1, COX-2, and TNF-α in the mouse cerebral cortex. Our findings introduce a bioactive compound from natural products that decreases proinflammatory factor production and has application for the treatment of neurodegenerative diseases.

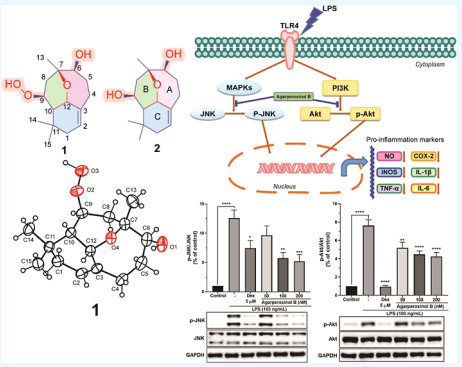

INTRODUCTION

Agarwood is a precious fragrant resin produced in the heartwood of several *Aquilaria* trees in the Thymelaeaceae family that can promote the healing of wounds from injuries.[1] Agarwood is primarily used as incense and its essential oil is in high demand in the perfume industry, as evidenced by the recent development of novel consumer products, such as agarwood essence, soap, and shampoo.[2] Agarwood has also been used in folk medicine in Southeast Asia as a sedative and an analgesic medication,[3] as well as for the treatment of inflammation-related diseases, such as rheumatism, arthritis, and asthma.[4]

Microglia are known as resident immune cells of the central nervous system (CNS) and are associated with several serious medical conditions in brain inflammatory immune and degenerative processes, such as Alzheimer's and Parkinson's disease.[5] Neuroinflammation can be caused by the activation of microglial cells and the subsequent release of several important mediators, including NO, PGE2, TNF-α, interleukin (IL-1β, IL-6), and express COX-2 enzyme and iNOS enzyme, during the inflammation process that is involved in neurodegenerative disorders.[5a,6] LPS-stimulated microglial cells have become one of the most commonly used means of releasing several inflammatory mediators into several cell types.[7] For most of the aforementioned conditions, no satisfying treatment of the associated inflammation is available. Currently, general treatment relies on the use of conventional anti-inflammatory drugs such as steroidal and nonsteroidal drugs (NSAIDs), which have several adverse effects and can be used to treat acute and chronic inflammatory disorders. Thus, it is necessary to develop safe, novel anti-inflammatory drugs from natural products that do not cause any side effects. For this reason, the search for novel anti-inflammatory drugs remains an important field in drug discovery.

Phytochemical studies of agarwood were first performed during the 1980s and 1990s and have recently been rapidly increasing in number. Among thirteen species reported as fragrant resin producers,[1,4] four (*Aquilaria sinensis*, *Aquilaria crassna*, *Aquilaria malaccensis*, and *Aquilaria filaria*) have been widely investigated, and more than 182 sesquiterpenoids and 240 chromone derivatives have been identified from agarwood thus far.[8] Our preliminary research results led us to biologically screen active compounds with anti-inflammatory effects in vitro.[9] During our ongoing search for bioactive and structurally interesting sesquiterpenoids from *A. malaccensis*, we recently reported several compounds possessing unusual structural

Received: August 7, 2023
Revised: October 18, 2023
Accepted: October 26, 2023
Published: November 9, 2023

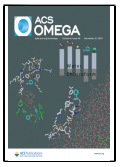

scaffolds.[10] Further chemical investigation of the ether fraction of this plant led us to isolate a novel tricyclic 6/6/7 carbon framework. Herein, we present a study on the isolation and structural elucidation of agarperoxinols A and B (Figure 1),

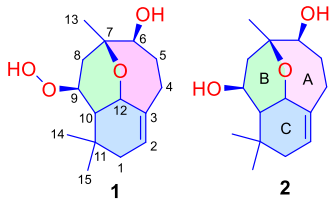

Figure 1. Chemical structure of compounds **1** and **2**.

novel rearranged humulene-type sesquiterpenoids, along with a plausible biosynthetic pathway and results showing significant antineuroinflammatory activities in microglial BV2 cells. We evaluated the anti-inflammatory effect of agarperoxinol B using LPS-activated microglial cells and found a significant decrease in the levels of NO, TNF-α, IL-1β, and IL-6, as well as in the expression of iNOS and COX-2. We further investigated the effects of agarperoxinol B on the Akt and mitogen-activated protein kinases (MAPK) signaling pathways to elucidate the underlying inhibitory mechanism. Finally, agarperoxinol B showed an anti-inflammatory effect in an LPS-treated mouse model. These results provide positive data on the potential of agarperoxinol B as an anti-inflammatory drug from a natural product.

RESULTS AND DISCUSSION

Agarperoxinol A (**1**) was isolated as colorless needles (petroleum ether-ethyl acetate, 5:1, v/v) with specific optical rotation $[\alpha]_D^{20}$ −28.1 (*c* 0.1, MeOH). The molecular formula was determined as $C_{15}H_{24}O_4$ from HRESI/TOF-MS by the positive ion peak at *m*/*z* 269.1745 $[M + H]^+$ (calcd for $C_{15}H_{25}O_4$, 269.1753), indicating 4 degrees of unsaturation. The ^{1}H NMR and HSQC data (Table 1) of **1** revealed the presence of an olefinic proton (δ_H 5.33, quint, J = 2.5 Hz, H-2); three oxymethines [(δ_H 4.25 (td, J = 6.5, 3.5 Hz, H-12), δ_H 4.22 (dt, J = 4.0, 2.5 Hz, H-9), and δ_H 3.50, t, J = 3.5 Hz, H-6)]; four methylene groups (δ_H 2.39−1.71); one methine (δ_H 1.56, dd, J = 6.5, 3.5 Hz, H-10); and three tertiary methyl groups (δ_H 1.41, 1.02, and 0.96). The ^{13}C NMR spectrum of **1** contained 15 carbon signals corresponding to a pair of olefinic carbons (δ_C 140.6, and 122.1); four oxygenated carbons (δ_C 79.5, 76.1, 74.3, and 70.7); and one quaternary carbon (δ_C 33.5). Consideration of the downfield chemical shift of C-9 (δ_C = 79.5) and a broad singlet of the ^{1}H NMR signal at δ_H = 7.73 in conjunction with the molecular formula suggested the presence of a free hydroperoxide group (−OOH) in the structure of **1**. Based on the aforementioned data, the existence of one double bond accounted for one degree of unsaturation, and the remaining three degrees of unsaturation demonstrated that **1** had a tricyclic skeleton. The ^{1}H−^{1}H COSY data of **1** showed correlations of the three-spin coupling systems H_2-1/H-2, H_2-4/H_2-5/H-6, and H_2-8/H-9/H-10/H-12, as shown in Figure 2. The key HMBC correlations were observed from H_2-4 to C-3/C-5/C-6/C-12 and from H-12 to C-3/C-7/C-9, which when considered in conjunction with the ^{1}H−^{1}H COSY correlations indicated the existence of a 7-membered carbon ring (A ring, Figure 1). In addition, two six-membered B- and C-rings were established by the HMBC cross peak from H_2-8

Table 1. ^{1}H and ^{13}C NMR Spectroscopic Data of Agarperoxinol A (1) and B (2) in $CDCl_3$

	agarperoxinol A (**1**)[a]		agarperoxinol B (**2**)[b]	
no.	δ_H (J in Hz)	δ_C	δ_H (J in Hz)	δ_C
1a	1.84 d (14.5)	36.1	1.91 d (20.0)	36.2
1b	1.71 dt (14.5, 3.5)		1.71 m	
2	5.33 quint (2.5)	122.1	5.30 dt (4.8, 2.4)	122.0
3		140.6		139.7
4a	2.39 m	27.6	2.40dddd (11.2, 10.4, 6.4, 3.2)	27.8
4b	2.08 dd (12.5, 4.0)		2.10ddd (11.2, 6.4, 4.8)	
5a	1.95ddd (11.0, 8.0, 3.5)	34.6	1.96 dtd (10.4, 6.4, 4.8)	32.7
5b	1.72ddd (11.0, 7.0, 3.5)		1.66tdd (10.4, 6.4, 3.2)	
6	3.50 t (3.5)	74.3	3.69 m	73.6
7		76.1		76.6
8a	2.10 dd (15.5, 2.5)	30.4	2.09 dd (14.4, 4.8)	39.1
8b	1.84 dd (15.5, 4.5)		1.48 dd (14.4, 5.6)	
9	4.22 dt (4.0, 2.5)	79.5	4.02 q (5.6)	65.5
10	1.56 dd (6.5, 3.5)	47.0	1.61 t (5.6)	52.4
11		33.5		33.8
12	4.25 td (6.5, 3.5)	70.7	4.30ddd (5.6, 4.0, 2.4)	71.9
13	1.41 s	27.2	1.35 s	26.1
14	1.02 s	27.2	1.10 s	28.5
15	0.96 s	28.2	0.95 s	28.5
9-OOH	7.73 br s			

[a]Data were measured at 500 MHz (^{1}H) and 125 MHz (^{13}C). [b]Data were measured at 800 MHz (^{1}H) and 200 MHz (^{13}C).

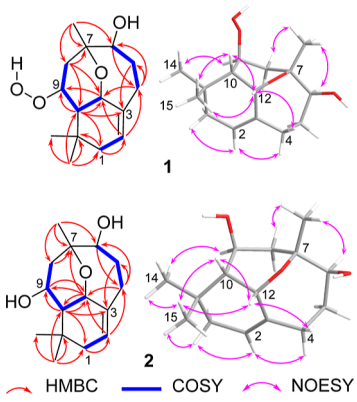

Figure 2. Key HMBC, ^{1}H−^{1}H COSY, and NOESY correlations of **1** and **2**.

to C-7/C-10/C-12 and from H-10 to C-1/C-3/C-4/C-9/C-11/C-12, which was supported by the ^{1}H−^{1}H COSY correlations of H_2-8/H-9/H-10/H-12. It was inferred from these data that the A-ring was fused with the B-ring through an ether bridge from C-7 to C-12 and that the B-ring was connected to the C-ring via a carbon bridge between C-10 and C-12. Thus, the planar structure of **1** was assigned as a tricyclic 6/6/7 rearranged humulene-type sesquiterpenoid (Figure 2).

The relative configuration of **1** was interpreted based on its NOESY spectrum. NOESY correlations were observed among H-10/H-12, H-10/H_3-15, H-12/H_3-15, and H-12/H-4a, suggesting that H-4a, H-10, H-12, and H_3-15 were in the β-orientation. However, NOESY cross-peaks were observed among H_2-1/H_3-14, H_2-1/H-2, H-2/H-4b, and H-9/H_3-14, indicating that H_2-1, H-2, H-4b, H-9, and H_3-14 were on the opposite side of the molecule and therefore in the *a*-

https://doi.org/10.1021/acsomega.3c05783
ACS Omega 2023, 8, 43873−43882

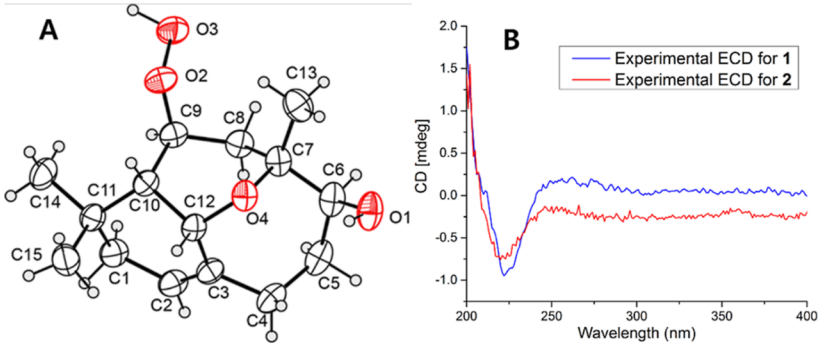

Figure 3. (A) X-ray crystallographic structure of **1**. (B) Comparison of the observed ECD spectral data of **1** and **2**.

orientation. The absolute configuration of **1** was determined by single-crystal X-ray diffraction analysis with Cu Kα radiation (λ = 1.54184) and is shown in Figure 3A. Hence, the stereochemistry of **1** was unambiguously assigned as 6*S*,7*R*,9*S*,10*S*,12*S*.

Agarperoxinol B (**2**) was obtained as colorless needles (petroleum ether-ethyl acetate, 8:1, v/v) with specific optical rotation $[\alpha]_D^{20}$ + 108.3 (*c* 0.12, MeOH). The molecular formula of **2** was deduced as $C_{15}H_{24}O_3$ on the basis of a protonated ion peak at *m*/*z* 253.1808 $[M + H]^+$ (calcd for $C_{15}H_{25}O_3$, 253.1804), which implied 4 degrees of unsaturation. The loss of 16 mass units of **2** compared with the molecular weight of **1** indicated the absence of an oxygen atom in the structure of **2**. The 1D NMR data of **2** (Table 1) were similar to those of **1**, demonstrating that **2** possessed the same 6/6/7 tricyclic core framework as **1** (Figure 1). However, **2** differed from **1** in that a free hydroperoxide group in **1** was replaced by a hydroxyl group at C-9 in **2**. The chemical shift of C-9 at δ_C 79.5 in **1** was upfield-shifted in **2** to δ_C 65.5, whereas the chemical shifts of C-8 at δ_C 30.4 and C-10 at δ_C 47.0 in **1** were downfield-shifted at δ_C 39.1 and δ_C 52.4, respectively. The HMBC correlations from H-9 to C-7/C-10/C-11/C-12, from H-10 to C-1/C-3/C-9/C-11/C-12/C-14/C-15, and from H-12 to C-2/C-3/C-7/C-9/C-10 confirmed the existence of an oxygen bridge between C-7 and C-12 and a carbon bridge between C-10 and C-12. The relative configuration of **2** was deduced from the NOESY correlations. The orientations of protons H_2-1, H-2, H-9, H-10, H-12, H_3-14, and H_3-15 were assigned to those of **1** (Figure 2) by the key NOESY correlations. Due to sample scarcity and the low-quality single crystal obtained for compound **2**, the absolute configuration of **2** was further identified by experimental ECD spectral analysis (Figure 3B). The observed ECD spectral data of **2** were highly identical to those of **1**, and the absolute configuration of **2** was unambiguously determined to be 6*S*,7*R*,9*S*,10*S*,12*S*, namely, agarperoxinol B.

To the best of our knowledge, agarperoxinols A (**1**) and B (**2**) are represented as rearranged humulene-type sesquiterpenoids with an unprecedented tricyclic 6/6/7 scaffold for the first time here. In particular, compound **1**, with a free hydroperoxide functionality in its structural framework, is unique and rarely occurs in natural product metabolites. A plausible biosynthetic pathway for the agarperoxinols A and B is postulated to originate from the most common precursor farnesyl pyrophosphate (Scheme 1).[11] The humulyl cation might undergo hydrogenation and oxidation to produce the intermediate precursor 12-hydroxyhumula-2*Z*,6*E*,9*E*-triene, isolated from the same plant.[10] The intermediates could be

Scheme 1. Plausible Biosynthetic Pathway of 1 and 2

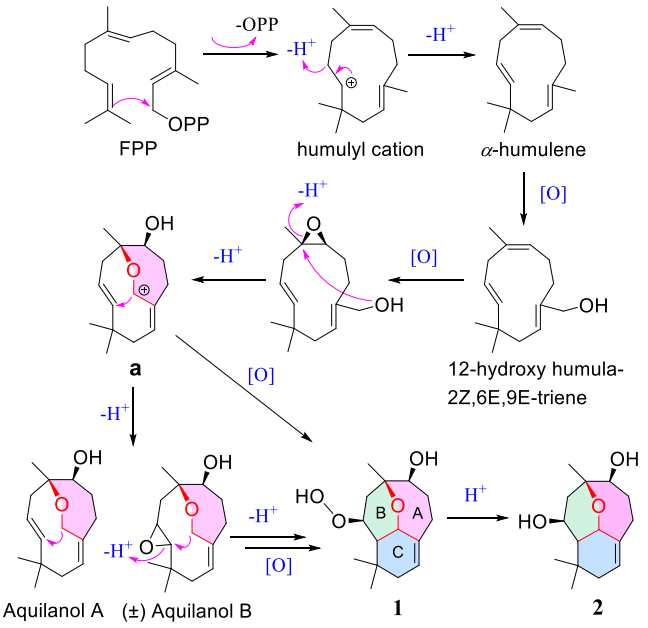

oxidized, dehydrated, and then converted to a carbocation (**a**) and deprotonated to produce the aquilanols A and B, humulene-type sesquiterpenoid 7/10 ring systems that have been reported in our previous studies.[10] Interestingly, the first precise synthesis of the naturally occurring aquilanols A and B was accomplished via (−)-caryophyllene oxide by retrocycloisomerization,[12] which demonstrated the feasibility of the total synthesis of agarperoxinols A and B by our putative biosynthetic pathways. Finally, the cyclization and oxidation of the intermediate precursor carbocation (**a**) generate a modified six-membered ring (the B- and C-rings) to afford the unprecedented 6/6/7 tricyclic skeleton.

Lipopolysaccharide (LPS) stimulates BV-2 microglia to release proinflammatory mediators, such as NO, TNF-α, IL-6, and PGE2, along with other key enzymes, cyclooxygenases, and COX-2, which are important mediators in CNS inflammatory diseases.[6b,7] Resinous woods from *Aquilaria* trees have long been used as a herbal drug in traditional medicine in most countries in the Indomalesian region for the treatment of inflammation, such as rheumatism, arthritis, analgesics, sedatives, and anxiety.[4] Considering the use of agarwood in traditional medicine remedies, we isolated the active components of agarwood and then used an LPS-stimulated microglial cell model to confirm the in vitro and in vivo anti-inflammatory effects of the isolated compounds. To

https://doi.org/10.1021/acsomega.3c05783
ACS Omega 2023, 8, 43873−43882

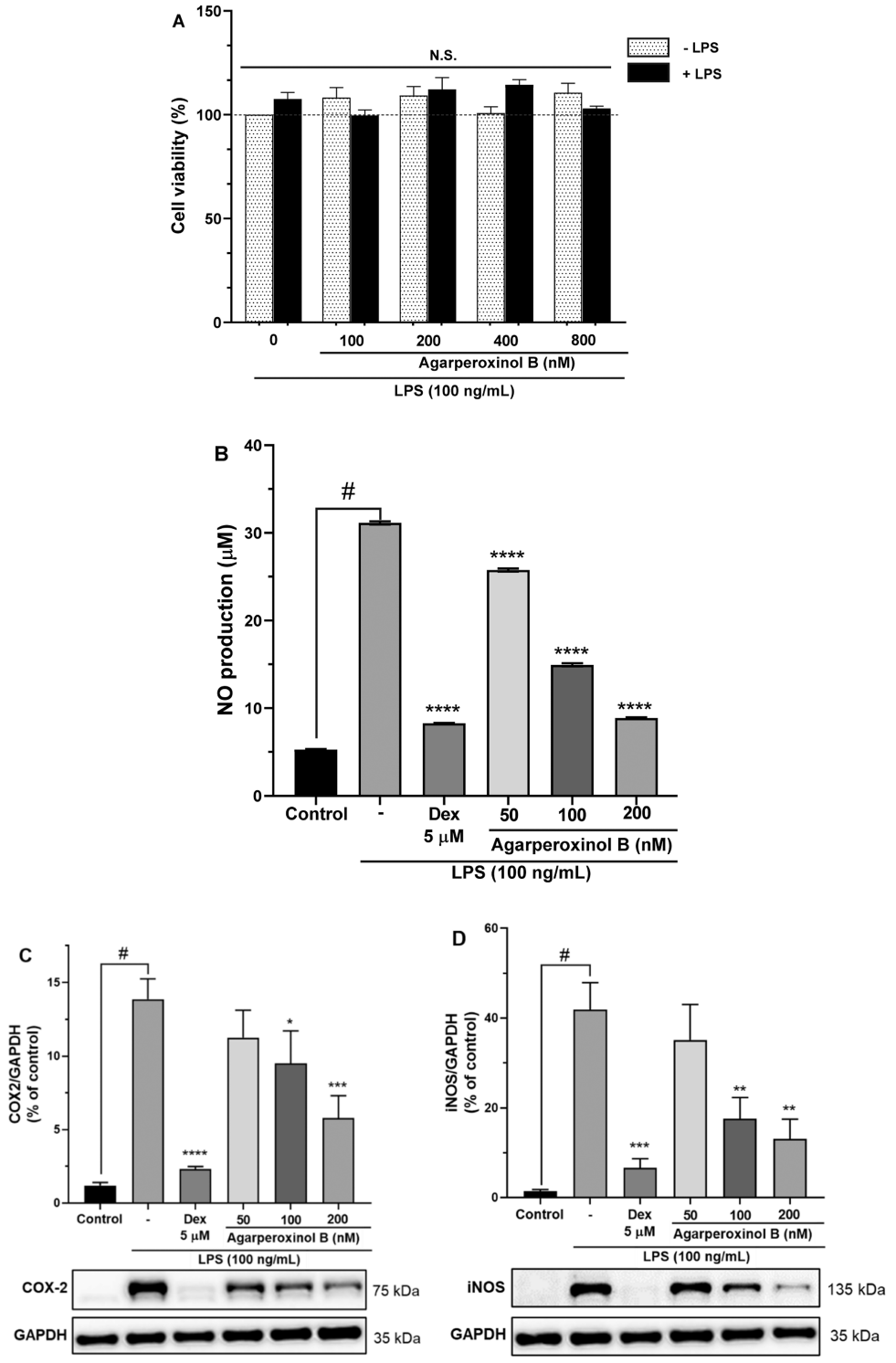

Figure 4. (A) Cell viability of compound **2** stained by EZ-Cytox for 30 min with absorbance determined at 450 nm; results are the percentage of the control group (n = 5, N.S. not significant). (B) Effect of compound **2** on LPS-induced NO production in microglial BV2 cells (n = 3). The inhibition of (C) COX-2 and (D) iNOS protein expressed by agarperoxinol B on LPS-activated microglial cells. Protein levels were determined using western blot analysis. The relative intensity of iNOS/COX-2 to GAPDH bands was calculated by densitometry (n = 5). The data are presented as mean ± SEM $^{\#}p < 0.0001$ was compared with a sample of the control group. $^{*}p < 0.05$, $^{**}p < 0.01$, $^{***}p < 0.001$, and $^{****}p < 0.0001$ were compared with the LPS group.

gather more mass for agarperoxinol compounds (**1** and **2**), isolation from the extract was performed again, but only **2** was successful. Agarperoxinol A (**1**) possessed the free peroxide group, and it could be transformed into agarperoxinol B (**2**), which can implicate that the structure of agarperoxinol B is more stable rather than agarperoxinol A. The isolated mass of **1** was not sufficient for further biological activity. Thus, only the chemical information on the novel compound **1** in this study and novel compound **2** was used for further biological study.

https://doi.org/10.1021/acsomega.3c05783
ACS Omega 2023, 8, 43873−43882

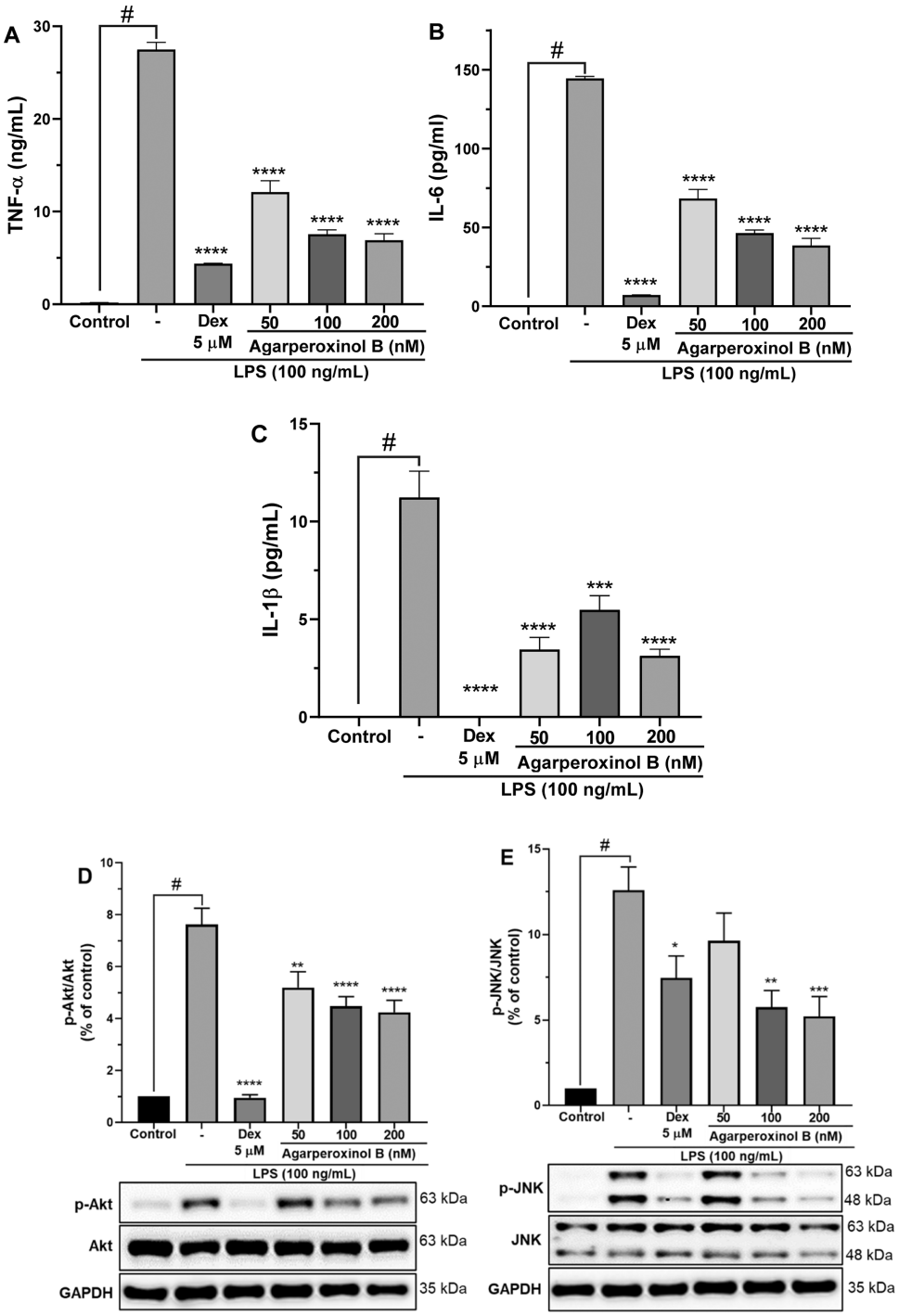

Figure 5. (A) TNF-α, (B) IL-6, and (C) IL-1β levels in the medium were determined using an ELISA kit; values are mean ± SEM of three independent experiments. The inhibition of (D) Akt and (E) JNK phosphorylation protein expressed by agarperoxinol B on LPS-activated microglial cells. Protein levels were determined by using western blot analysis. The relative intensity of p-Akt/Akt and p-JNK/JNK bands were calculated by densitometry. The data were presented as mean ± SEM (n = 5). $^{\#}p < 0.0001$ was compared with the sample of the control group. $^{*}p < 0.05$, $^{**}p < 0.01$, $^{***}p < 0.001$, and $^{****}p < 0.0001$ were compared with the LPS group.

The cytotoxicity of agarperoxinol B was determined in the presence or absence of LPS by a colorimetric assay with the EZ-Cytox reagent. The viability of cells treated with agarperoxinol B at 0, 100, 200, 400, and 800 nM were 100 ± 0.0, 99.68 ± 2.62, 112.19 ± 5.70, 114.37 ± 2.55, and 103.05 ± 1.12%, respectively. The viability of cells treated with agarperoxinol B at 0, 100, 200, 400, and 800 nM in the presence of LPS (100 ng/mL) were 107.54 ± 3.20, 108.28 ± 4.79, 109.22 ± 4.34, 100.76 ± 3.04, and 110.54 ± 4.59%, respectively. The viability of BV2 microglial cells did not decrease upon treatment with agarperoxinol B alone or cotreatment with agarperoxinol B and LPS (100 ng/mL). The aforementioned data showed that agarperoxinol B displayed no significant cytotoxicity to BV2 microglial cells at fourfold the effective dose (Figure 4A).

https://doi.org/10.1021/acsomega.3c05783
ACS Omega 2023, 8, 43873−43882

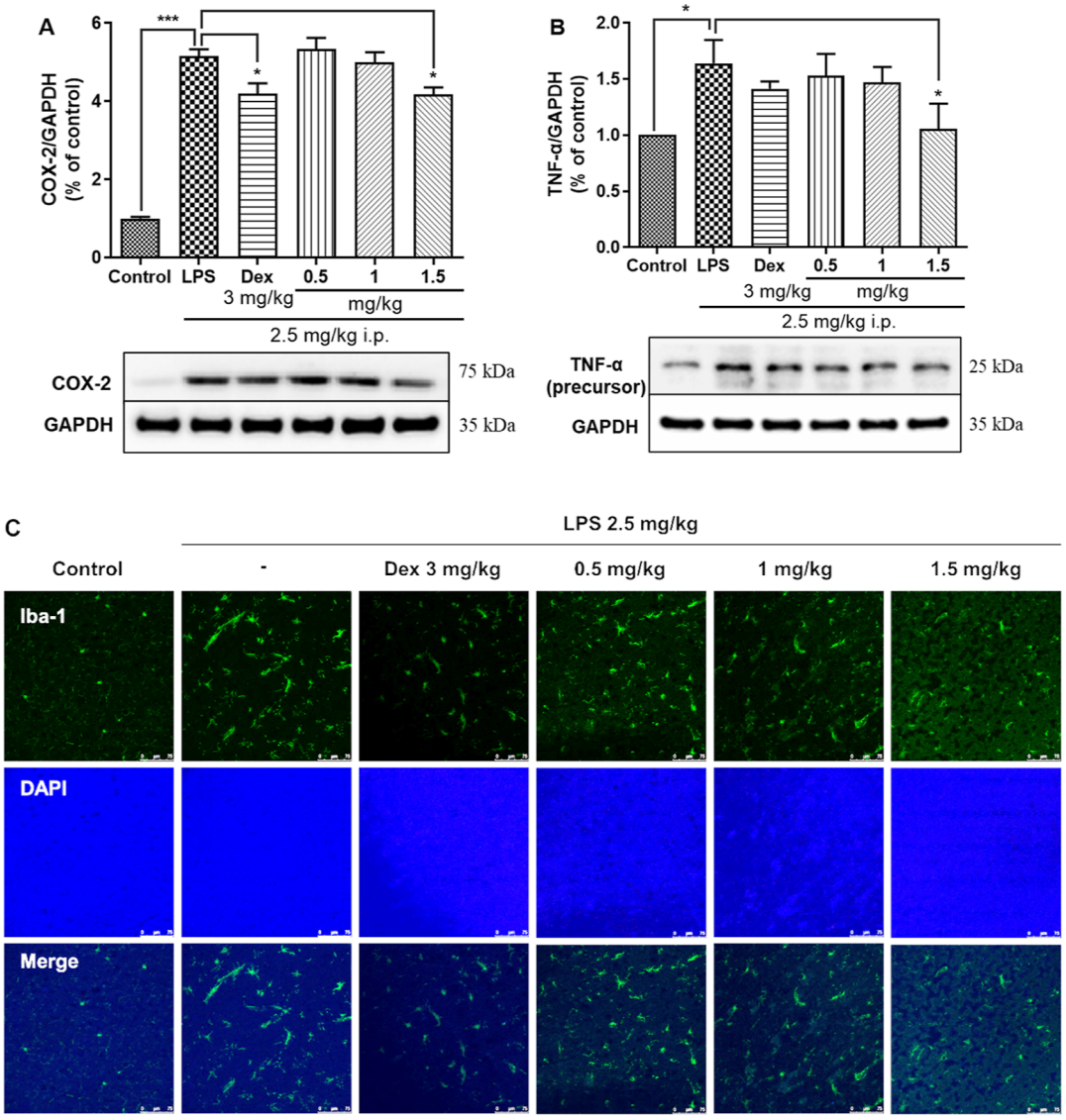

Figure 6. Agarperoxinol B and dexamethasone (3 mg/kg) inhibit the expression of COX-2 and TNF-α in LPS-treated mice, (A) COX-2 (n = 6) and (B) TNF-α (n = 6) levels in the mouse cortex were detected by western blotting. Agarperoxinol B and dexamethasone (3 mg/kg) precluded the activation of microglia and astrocytes in LPS-treated mice. (C) Iba-1 was detected by an immunofluorescence assay (n = 3), scale bar = 75 μm. The data are expressed as the mean ± SEM. *p < 0.05 and ***p < 0.001 were compared with the control group and the LPS group.

NO is a signaling molecule that plays a key role in the pathogenesis of inflammation and can act as a defense and regulatory molecule with homeostatic activities but is pathogenic when produced in excess.[13] In recent years, NO-releasing drugs have been developed, usually as derivatives of other drugs, that exhibit powerful anti-inflammatory effects. In our target deconvolution experiments, cells were treated with serial dilutions of agarperoxinol B at concentrations of 50, 100, and 200 nM for 1 h and then cotreated with LPS (100 ng/mL). The corresponding levels of NO production in the culture medium were 25.77 ± 0.10, 14.94 ± 0.10, and 8.87 ± 0.05 μM (Figure 4B). In this study, the NO production in the treated cells differed significantly from those in the negative and positive controls (dexamethasone, Dex 5 μM) of 31.14 ± 0.10 and 8.26 ± 0.04 μM (p < 0.0001), respectively. Interestingly, these results revealed that agarperoxinol B significantly inhibited NO production in LPS-stimulated BV2 microglial cells in a dose-dependent manner with an IC_{50} value of 110.8 ± 2.0 nM.

Western blotting was used to determine whether agarperoxinol B also regulated the expression of COX-2 and iNOS enzymes in LPS-induced microglial BV2 cells (Figure 4C,D). The results showed that the treatment of microglial BV2 cells with agarperoxinol B in the presence of LPS (100 ng/mL) for 24 h inhibited the expression of COX-2 and iNOS protein in a concentration-dependent manner. As shown in Figure 4C,D, treatment with agarperoxinol B at concentrations of 50, 100, and 200 nM significantly suppressed the protein expression of both COX-2 (81.0, 68.4, and 41.7%) and iNOS (83.9, 41.9, and 31.2%), whereas the group treated with only LPS had markedly enhanced levels of COX-2 and iNOS compared with the control group. These data suggest that agarperoxinol B both inhibited NO production and modulated COX-2 and iNOS expression levels in LPS-stimulated BV2 microglial cells.

The proinflammatory cytokine TNF-α itself can stimulate several functional cells to produce other proinflammatory mediators, including NO, IL-1β, and IL-6.[14] Accordingly, we examined the effect of agarperoxinol B on LPS-induced

https://doi.org/10.1021/acsomega.3c05783
ACS Omega 2023, 8, 43873−43882

upregulation of TNF-α, IL-6, and IL-1β by determining their secretory concentration in cell culture media using specific enzyme-linked immunosorbent assay (ELISA) kits. As shown in Figure 5A−C, the secretion of TNF-α, IL-6, and IL-1β was significantly upregulated by stimulation with LPS. However, the proinflammatory cytokines were remarkably inhibited in a dose-dependent manner by treatment with agarperoxinol B, which at concentrations of 50, 100, and 200 nM highly significantly decreased the production of TNF-α (44.0, 27.5, and 25.1%, respectively), IL-6 (47.3, 32.1, and 26.6%, respectively), and IL-1β (30.7, 48.8, and 27.8%, respectively) compared with that of the LPS group.

Toll-like receptors (TLRs) belong to a broad family of proteins that function in the innate immune system to recognize invading pathogens that produce an inflammatory immune response.[15] Among the TLR family, toll-like receptor 4 (TLR4) is recognized as the cell−surface receptor for LPS and plays an important role in the initiation of the inflammatory immune response.[16] The activation of TLR4 is implicated in the activation of downstream inflammatory signaling pathways, including the activation of MAPKs, nuclear factor-kappa B (NF-κB), and phosphatidylinositol 3-kinase/protein kinase B (PI3K-Akt),[17] which induces the production of inflammatory mediators such as NO, proinflammatory cytokines, iNOS, and COX-2.[16b,18] To verify whether agarperoxinol B is involved in LPS-induced activation of Akt and MAPK signaling pathways in microglial, western blotting was performed on phosphorylated forms of Akt, JNK, and p38, and the results are shown in Figure 5D,E, and Supporting Information Figure S21. We found that phosphorylation of Akt and JNK was strongly increased in LPS-stimulated microglial cells, whereas phosphorylation of Akt and JNK was significantly decreased in a dose-dependent manner when the cells were treated with agarperoxinol B after LPS activation. However, western blot analysis of p38 MAPK phosphorylation did not show any significant inhibition of the protein expression when compared with that of LPS-activated microglial cells (Supporting Information Figure S21). Our findings suggest that the anti-inflammatory properties of agarperoxinol B in LPS-activated microglia are probably attributable to its inhibition of the LPS-stimulated activation of Akt and JNK in MAPK signaling pathways. Therefore, the Akt and JNK/MAPK signaling pathways may be considered as one of the mechanisms in regulating inflammatory activity of agarperoxinol B.

To further determine whether agarperoxinol B can inhibit proinflammatory factors in the mouse brain, we used a mouse model intraperitoneally injected with LPS at 2.5 mg kg^{-1} day^{-1} according to a previous study:[19] Western blot analysis indicated significant overexpression of COX-2 and TNF-α in the mouse cortex, as shown in Figure 6A,B. A positive control, dexamethasone, showed antineuroinflammatory activity in vitro at 5 μM and significantly inhibited the expression of the proinflammatory mediators NO, iNOS, COX-2, TNF-α, IL-1β, and IL-6.[16b,20] Mice treated orally with agarperoxinol B also showed significantly reduced expression of proinflammatory factors, including COX-2 and TNF-α, in the mouse cerebral cortex. These data suggest that agarperoxinol B may prevent neuroinflammation by inhibiting proinflammatory factors, such as COX-2 and TNF-α.

To assess whether agarperoxinol B inhibits neuroinflammation, we used the immune cell marker Iba-1, which is upregulated in reactive microglia and often used to visualize these cells.[21] To confirm that Iba-1 was affected by treatment with agarperoxinol B, we performed an immunofluorescence assay to observe Iba-1 positive cells in mouse cortex brains. Consistent with the western blot data, histological Iba-1 immunoreactivity was detected, as shown in Figure 6C, which clearly demonstrated that LPS induced higher levels of Iba-1 than the control treatment. In contrast to the LPS-treated group, cotreatment with agarperoxinol B clearly attenuated the expression of Iba-1. This finding indicated that agarperoxinol B may inhibit neuroinflammation in an LPS-treated mouse model.

CONCLUSIONS

In summary, continuing studies on agarwood chips from *A. malaccensis* led to the isolation of two unprecedented framework 6/6/7 humulene-type sesquiterpenoids, agarperoxinols A and B. The precise structures of these novel compounds were elucidated by using extensive NMR data. The absolute configuration of agarperoxinol A was determined by single-crystal X-ray crystallographic analysis, whereas the absolute configuration of agarperoxinol B was assigned by experimental ECD spectral analysis and comparison with the data for agarperoxinol A.

In vitro screening of anti-inflammatory targets from the agarwood of *A. malaccensis* showed that agarperoxinol B intensively inhibited NO production in LPS-treated BV2 microglial cells. To demonstrate the pharmacological activity of agarperoxinol B against LPS-induced neuroinflammatory responses and elucidate the underlying molecular signaling mechanisms, we treated COX-2 and iNOS proteins with agarperoxinol B and investigated by western blot analysis. The results showed that agarperoxinol B reduced the expression of iNOS and then decreased NO production and strongly downregulated the expression of COX-2 in a dose-dependent manner. Investigation of the expression and secretion of key proinflammatory factors, including TNF-α, IL-6, and IL-1β, showed significantly decreased levels after treatment with agarperoxinol B in the presence of LPS. To further explore the underlying mechanism of the inhibitory effects of agarperoxinol B on LPS-stimulated microglial cells, we investigated the signaling pathway related to the production of inflammatory mediators, where both Akt and MAPK pathways were evaluated. Agarperoxinol B severely attenuated the phosphorylation of Akt and JNK but did not significantly inhibit p38 MAPK. In an in vivo study, agarperoxinol B also significantly suppressed the expression of microglial markers Iba-1, COX-2, and TNF-α in an LPS-treated mouse model. This finding provided further evidence that agarperoxinol B inhibited the activation of microglia in the LPS-injected mouse model. Therefore, the abovementioned data demonstrate the potential of agarperoxinol B as a novel therapeutic agent for neuroinflammatory disorders. Although the present and earlier findings demonstrate the potential beneficial effects of agarperoxinol B in modulating microglial activation, signaling pathways have many targets, and the action of agarperoxinol B regarding upstream and downstream targets needs further investigation.

EXPERIMENTAL SECTION

General Experimental Procedures. Melting points were determined by using a Mitamura Riken melting point apparatus (Japan). The optical rotations were measured on a

https://doi.org/10.1021/acsomega.3c05783
ACS Omega 2023, 8, 43873−43882

JASCO P-2000 polarimeter (Japan) at 20 °C. IR spectrum was obtained from JASCO FT/IR 4200 (Japan). The ultraviolet (UV) and ECD spectra were measured on a Chirascan-plus instrument (Applied Photophysics Ltd., UK). NMR spectra were recorded on a Bruker ASCEND (800 MHz) and Bruker ADVANCE 500 MHz FT-NMR spectrometer (Germany). NMR solvents were purchased from Sigma-Aldrich (USA). HR-ESIMS were measured on an Agilent 6350 Q-TOF mass spectrometer (Agilent, USA). The X-ray crystallographic data were carried out on an Agilent SuperNova CCD detector system with Cu Kα radiation (λ = 1.54184 Å). LC analyses were carried out using an Agilent 1260 Infinity System (USA) with a Phenomenex Luna 100 RP-C18 (250 mm × 4.6 mm i.d., 5 μm) column equipped with an autosampler, DAD, and column thermostat. Semipreparative HPLC was performed using a Gilson 321 pump and Gilson UV/vis-155 detector system (Gilson, Middleton, USA) with a Phenomenex Luna 100 RP-C18 (250 × 10 mm i.d., 5 μm) column. Column chromatography was performed using silica gel 60 (0.040−0.063 mm; Merck, Germany) and Sephadex LH-20 (Amersham Bioscience AB, Uppsala, Sweden) as stationary phase. All solvents used for isolation were purchased from Duksan Pure Chemical Co. (Gyeonggi-do, Korea). Solvents for HPLC were provided by J.T. Baker (USA).

Plant Material, Extraction, and Isolation Methods. Plant materials, extraction, and isolation methods are presented in the Supporting Information file.

Agarperoxinol A (1). Colorless needle crystal (PE/EtOAc 5:1); mp 156−158 °C; $[\alpha]_D^{20}$ −28.1 (*c* 0.14, MeOH); UV (MeOH); λ_{max} (log ε): 227 (5.01); ^{1}H NMR and ^{13}C NMR data: see Table 1; HR-ESIMS *m*/*z* 269.1745 $[M + H]^+$ (calcd for $C_{15}H_{25}O_4$, 269.1753).

Crystallographic data of agarperoxinol A (**1**) for $C_{15}H_{24}O_4$ (M = 268.34 g/mol): monoclinic, space group $P2_1/n$ (no. 14), a = 8.9468(3) Å, b = 16.8211(6) Å, c = 10.2017(4) Å, β = 109.839(4), V = 1444.19(9) Å^3, Z = 4, T = 291(6) K, μ(Cu Kα) = 0.715 mm^{-1}, D_{calc} = 1.234 g/cm^3, 15,045 reflections measured (10.518 ≤ 2θ ≤ 153.188), 2999 unique (R_{int} = 0.0527, R_{sigma} = 0.0259) which were used in all calculations. The final R_1 was 0.0447 ($I > 2\sigma(I)$) and wR_2 was 0.1393 (all data). A suitable crystal was selected and measured on a SuperNova, Dual, Cu at zero, AtlasS2 diffractometer. The crystal was kept at 291.0(6) K during data collection. Using Olex2,[22] the structure was solved with the SHELXT.[23] Structure solution program using direct methods and refined with the SHELXL[24] refinement package using least squares minimization. Crystallographic data have been deposited at the Cambridge Crystallographic Data Centre (**1**: CCDC, 2194681). Copies of the data can be obtained free of charge by application to the Director, CCDC, 12 Union Road, Cambridge CB2 1EZ, UK (fax: +44-(0)1223-336,033 or e-mail: deposit@ccdc.cam.ac.uk).

Agarperoxinol B (2). Colorless needle crystal (PE/EtOAc 8:1); mp 148−150 °C; $[\alpha]_D^{20}$ + 108.3 (*c* 0.12, MeOH); UV (MeOH); λ_{max} (log ε): 208 (6.24), 227 (4.88); ^{1}H NMR and ^{13}C NMR data: see Table 1; HR-ESIMS *m*/*z* 253.1808 $[M + H]^+$ (calcd for $C_{15}H_{25}O_3$, 253.1804).

Biological Reagents. LPS (*Escherichia coli*, 0111:B4), dimethyl sulfoxide (DMSO), sulfanilamide, *N*-(1-naphthyl)-ethylenediamine dihydrochloride, and sodium nitrite were purchased from Sigma-Aldrich (St. Louis, MO, USA). All primary antibodies including those against iNOS (#13120), COX-2 (#12282), dehydrogenase (GAPDH) (#2118), Akt (#4685), p-Akt (Ser473) (#4060), JNK (#9258), p-JNK (#4668), p-38 (#9212), p-p38 (#9211), TNF-α (#3707), and Iba1/AIF-1 (#17198), as well as the antirabbit horseradish peroxidase (HRP)-linked IgG (#7074) antibodies were purchased from Cell Signaling Technology (Beverly, MA, USA).

Cell Culture and Viability. The BV2 cells were provided by S.J.L. (Seoul National University, Seoul, Korea). Cells were cultured and maintained in Dulbecco's Modified Eagle Medium F12 (DMEM-F12, Gibco, Grand Island, NY, USA) supplemented with 5% heat-inactivated fetal bovine serum (Gibco, Grand Island, NY, USA) and 1% penicillin/streptomycin in a 5% CO_2 incubator at 37 °C. To evaluate the percentage of cell viability, cells (5.0×10^4) were seeded into 96-well plates and incubated for 24 h at 37 °C. The cells were then treated with various concentrations of compounds (50, 100, and 200 nM) in the presence or absence of LPS for 24 h. EZ-Cytox reagent (Daeil Lab Co. Ltd., Seoul, Republic of Korea) was used to detect cell viability. The absorbance at 450 nm was measured using a microplate absorbance reader (Multiskan SkyHigh, Thermo Scientific, USA).

Animal Experiment. Male C57BL/6N mice (7 weeks old) weighing 25−28 g were purchased from Orient Bio Inc. (Seongnam, Korea) and were kept in a room controlled for temperature (23 ± 2 °C) and humidity (50 ± 10%) under a 12 h light−dark cycle (light on from 06:00 to 18:00 h) with food and water available ad libitum. These experimental protocols were approved by the Sejong Animal Care Committee and performed according to the regulations of the Korean Council on Animal Care (no. SJ-20210701).

Mice were randomly divided and numbered into six groups (six mice per group) as follows: (1) vehicle [saline with 1% DMSO, per oral (po)] treatment normal control group, (2) LPS (2.5 mg/kg/day, intraperitoneal injection) treatment control group, (3) dexamethasone (3 mg/kg/day, po) and LPS treatment group (positive control group), (4) agarperoxinol B (0.5 mg/kg/day, po) and LPS treatment group, (5) agarperoxinol B (1 mg/kg/day, po) and LPS treatment group, and (6) agarperoxinol B (1.5 mg/kg/day, po) and LPS treatment group. LPS, dexamethasone, and agarperoxinol B were dissolved in saline with 1% DMSO. Mice were orally treated with dexamethasone and agarperoxinol B for 8 consecutive days. LPS was injected from the sixth day to the eighth day 30 min after dexamethasone and agarperoxinol B treatment. After 30 min LPS injection on the eighth day, the brain cortex was collected and then stored at −80 °C.

Measurement of NO Production. The cells (5.0×10^5) were seeded into 6-well plates and incubated at 37 °C for 24 h, then pretreated with serially diluted concentrations of compounds (50, 100, and 200 nM) for 1 h, and then cotreated with LPS (100 ng/mL) for 24 h. The nitrite levels in the cultured media were measured using a colorimetric method based on the Griess reaction. In brief, 50 μL culture medium was added with an equal volume of mixed Griess reagents (1% sulfanilamide, 0.1% naphthyl ethylenediamine dihydrochloride, and 5% phosphoric acid), incubated at room temperature for 15 min. The absorbance was measured at 540 nm using a microplate reader (Multiskan SkyHigh, Thermo Scientific, USA). The concentration of nitrite was determined from the standard curve.

Enzyme-Linked Immunosorbent Assay. The culture medium was collected and centrifuged at 13,000 rpm for 5 min. The levels of IL-1β, IL-6, and TNF-α in the culture

https://doi.org/10.1021/acsomega.3c05783
ACS Omega 2023, 8, 43873−43882

medium were quantified using ELISA kits from R&D System Inc. (Minneapolis, MN, USA), according to the manufacturer's instructions.

Western Blot Analysis. The cells (5×10^5 cells/well) were seeded into a 6-well plate for 24 h, pretreated with various concentrations of compounds for 1 h, and then cotreated with LPS (100 ng/mL) for 24 h. Then, the cells were harvested and lysed using protein extraction buffers (PRO-PREP, iNtRON, Gyeonggi-do, Korea) and 1× phosphatase inhibitor cocktail III (PIC III, Merck, Darmstadt, Germany). Isolated brain tissues also were homogenized in PRO-PREP with phosphatase inhibitor cocktail III. The supernatants were collected after centrifuging at 13,000 rpm for 20 min at 4 °C. The total protein was quantified using Pierce BCA Protein Assay Kit (Thermo Scientific, Rockford, IL, USA) and calculated based on known concentrations of a BSA standard. The protein samples were loaded onto 10% SDS-polyacrylamide gels for electrophoresis separation and transferred to Immobilon-P polyvinylidene difluoride (Merck KGaA, Darmstadt, Germany) membranes, blocked with 5% BSA using blocking buffer solution (Double Blocker, T&I, Chuncheon, Korea) and incubated with the specific primary antibodies (1:1000) overnight at 4 °C. After washing with TBST, the membrane was incubated with the HRP-conjugated IgG secondary antibodies (1:2000) for 1 h at room temperature. The blots were detected using enhanced chemiluminescence reagents (Thermo Fisher Scientific Inc., Lafayette, CA, USA). Densitometry analysis of bands was performed using the FUSION Solo system (Vilber Lourmat, Collégien, France).

Immunofluorescence Assay. For immunohistochemistry, mouse brain tissues were fixed in 4% paraformaldehyde overnight at 4 °C. Fixed brain tissues were sectioned at 25 μm and preserved in a storage solution containing sucrose, phosphate buffer, and ethylene glycol at −20 °C. The brain sections were permeabilized using 0.5% Triton X-100 for 30 min and blocked using 5% BSA for 30 min. The sections were incubated with Iba-1 antibody (1:250) at room temperature. After 2 h of reacting, sections were incubated with Alexa Fluor 488-labeled IgG secondary antibody in the dark for 1 h. Then, sections were placed on slides, and cover glasses were mounted using a mounting medium containing DAPI. Images were acquired using a TCS SP5 confocal microscope (Leica, Mannheim, Germany).

■ ASSOCIATED CONTENT

Supporting Information

The Supporting Information is available free of charge at https://pubs.acs.org/doi/10.1021/acsomega.3c05783.

General experimental procedures, UV, OR, 1D/2D NMR and HR-ESIMS spectra of **1**−**2**, ECD calculations of **2** X-ray, and crystallographic data of **1** (PDF)

■ AUTHOR INFORMATION

Corresponding Author

Hyun Ok Yang − *Department of Integrative Biological Sciences and Industry & Convergence Research Center for Natural Products, Sejong University, Gwangjin-gu, Seoul 05006, Republic of Korea;* orcid.org/0000-0003-1604-0843; Phone: +82-02-3408-1959; Email: hoyang@sejong.ac.kr; Fax: +82-02-3408-4336

Authors

Chi Thanh Ma − *Faculty of Pharmacy, University of Medicine and Pharmacy at Ho Chi Minh City, Ho Chi Minh City 700000, Vietnam; Department of Integrative Biological Sciences and Industry & Convergence Research Center for Natural Products, Sejong University, Gwangjin-gu, Seoul 05006, Republic of Korea;* orcid.org/0000-0003-4058-3354

Sang Bin Lee − *Department of Integrative Biological Sciences and Industry & Convergence Research Center for Natural Products, Sejong University, Gwangjin-gu, Seoul 05006, Republic of Korea*

In Ho Cho − *Research Institute of Pharmaceutical Sciences, College of Pharmacy, Seoul National University, Gwanak-gu, Seoul 08826, Republic of Korea*

Jae Sik Yu − *Department of Integrative Biological Sciences and Industry & Convergence Research Center for Natural Products, Sejong University, Gwangjin-gu, Seoul 05006, Republic of Korea*

Tianqi Huang − *Korea Institute of Science and Technology (KIST) School, Korea University of Science and Technology (UST), Seongbuk-gu, Seoul 02792, Republic of Korea*

Tae Min Lee − *Department of Integrative Biological Sciences and Industry & Convergence Research Center for Natural Products, Sejong University, Gwangjin-gu, Seoul 05006, Republic of Korea*

Tu Loan Ly − *Faculty of Pharmacy, Ton Duc Thang University, Ho Chi Minh City, Ho Chi Minh City 700000, Vietnam*

Sung Won Kwon − *Research Institute of Pharmaceutical Sciences, College of Pharmacy, Seoul National University, Gwanak-gu, Seoul 08826, Republic of Korea;* orcid.org/0000-0001-7161-4737

Jeong Hill Park − *Research Institute of Pharmaceutical Sciences, College of Pharmacy, Seoul National University, Gwanak-gu, Seoul 08826, Republic of Korea;* orcid.org/0000-0003-3077-7673

Complete contact information is available at: https://pubs.acs.org/10.1021/acsomega.3c05783

Author Contributions

C.T.M.: Investigation, methodology, data analysis, validation, writing of original draft. S.B.L., I.H.C., T.H., T.M.L., T.L.L.: Methodology, data analysis, investigation. J.S.Y.: Review and editing of the manuscript. S.W.K., J.H.P., H.O.Y.: Funding acquisition, project administration, supervision, validation, writing review, and editing. All authors read and approved the final manuscript.

Notes

The authors declare no competing financial interest.

■ ACKNOWLEDGMENTS

This research was supported by the Rural Development Administration of Korea (PJ017031 & PJ017076) and by the Ministry of Science, ICT, and Future Planning through the National Research Foundation of Korea (2019K1A3A1A05088041). This work was also supported by a grant from the Vietnam National Foundation for Science and Technology Development (NAFOSTED) (grant number 108.05-2019.07).

■ ABBREVIATIONS

ECD, electronic circular dichroism; LPS, lipopolysaccharide; NO, nitric oxide; ELISA, enzyme-linked immunosorbent assay; TNF-α, tumor necrosis factor-α; IL-6, interleukin-6; IL-1β, interleukin-1 β; iNOS, inducible nitric oxide synthase; COX-2, cyclooxygenase-2; Akt, protein kinase B; JNK, C-jun N-terminal kinase; Iba-1, ionized calcium-binding adapter molecule 1; PGE2, prostaglandin E2; MAPK, mitogen-activated protein kinase; PI3K, phosphatidylinositol 3-kinase

■ REFERENCES

(1) Gao, M.; Han, X.; Sun, Y.; Chen, H.; Yang, Y.; Liu, Y.; Meng, H.; Gao, Z.; Xu, Y.; Zhang, Z.; et al. Overview of sesquiterpenes and chromones of agarwood originating from four main species of the genus Aquilaria. *RSC Adv.* **2019**, *9* (8), 4113−4130.

(2) Tajuddin, S. N.; Aizal, C. M.; Yusoff, M. M. Resolution of Complex Sesquiterpene Hydrocarbons in Aquilaria malaccensis Volatile Oils Using Gas Chromatography Technique. In *Agarwood: Science Behind the Fragrance*; Mohamed, R., Ed.; Springer Singapore, 2016; pp 103−124.

(3) Persoon, G. A.; van Beek, H. H. Growing 'The Wood of The Gods': Agarwood Production in Southeast Asia. In *Smallholder Tree Growing for Rural Development and Environmental Services: Lessons from Asia*; Snelder, D. J., Lasco, R. D., Eds.; Springer Netherlands, 2008; pp 245−262.

(4) Lee, S. Y.; Mohamed, R. The Origin and Domestication of Aquilaria, an Important Agarwood-Producing Genus. In *Agarwood: Science Behind the Fragrance*; Mohamed, R., Ed.; Springer Singapore, 2016; pp 1−20.

(5) (a) Perry, V. H.; Nicoll, J. A. R.; Holmes, C. Microglia in neurodegenerative disease. *Nat. Rev. Neurol.* **2010**, *6* (4), 193−201. (b) Yang, I.; Han, S. J.; Kaur, G.; Crane, C.; Parsa, A. T. The role of microglia in central nervous system immunity and glioma immunology. *J. Clin. Neurosci.* **2010**, *17* (1), 6−10. (c) Lull, M. E.; Block, M. L. Microglial Activation and Chronic Neurodegeneration. *Neurotherapeutics* **2010**, *7* (4), 354−365.

(6) (a) Medzhitov, R. Origin and physiological roles of inflammation. *Nature* **2008**, *454* (7203), 428−435. (b) Kim, Y. S.; Joh, T. H. Microglia, major player in the brain inflammation: their roles in the pathogenesis of Parkinson's disease. *Exp. Mol. Med.* **2006**, *38* (4), 333−347. (c) Li, H.; Li, M.-M.; Su, X.-Q.; Sun, J.; Gu, Y.-F.; Zeng, K.-W.; Zhang, Q.; Zhao, Y.-F.; Ferreira, D.; Zjawiony, J. K.; et al. Anti-inflammatory Labdane Diterpenoids from Lagopsis supina. *J. Nat. Prod.* **2014**, *77* (4), 1047−1053. (d) Liu, B.-Y.; Zhang, C.; Zeng, K.-W.; Li, J.; Guo, X.-Y.; Zhao, M.-B.; Tu, P.-F.; Jiang, Y. Anti-Inflammatory Prenylated Phenylpropenols and Coumarin Derivatives from Murraya exotica. *J. Nat. Prod.* **2018**, *81* (1), 22−33. (e) Gao, P.; Wang, L.; Zhao, L.; Zhang, Q.-y.; Zeng, K.-w.; Zhao, M.-b.; Jiang, Y.; Tu, P.-f.; Guo, X.-y. Anti-inflammatory quinoline alkaloids from the root bark of Dictamnus dasycarpus. *Phytochemistry* **2020**, *172*, 112260.

(7) Thameem Dheen, S.; Kaur, C.; Ling, E. A. Microglial activation and its implications in the brain diseases. *Curr. Med. Chem.* **2007**, *14* (11), 1189−1197.

(8) Li, W.; Chen, H.-Q.; Wang, H.; Mei, W.-L.; Dai, H.-F. Natural products in agarwood and Aquilaria plants: chemistry, biological activities and biosynthesis. *Nat. Prod. Rep.* **2021**, *38* (3), 528−565.

(9) Ma, C. T.; Ly, T. L.; Le, T. H. V.; Tran, T. V. A.; Kwon, S. W.; Park, J. H. Sesquiterpene derivatives from the agarwood of Aquilaria malaccensis and their anti-inflammatory effects on NO production of macrophage RAW 264.7 cells. *Phytochemistry* **2021**, *183*, 112630.

(10) Ma, C. T.; Eom, T.; Cho, E.; Wu, B.; Kim, T. R.; Oh, K. B.; Han, S. B.; Kwon, S. W.; Park, J. H. Aquilanols A and B, Macrocyclic Humulene-Type Sesquiterpenoids from the Agarwood of Aquilaria malaccensis. *J. Nat. Prod.* **2017**, *80* (11), 3043−3048.

(11) (a) Gutta, P.; Tantillo, D. J. Theoretical Studies on Farnesyl Cation Cyclization: Pathways to Pentalenene. *J. Am. Chem. Soc.* **2006**, *128* (18), 6172−6179. (b) Wang, S. C.; Tantillo, D. J. Prediction of a New Pathway to Presilphiperfolanol. *Org. Lett.* **2008**, *10* (21), 4827−4830.

(12) Maliori, A.; Athanasiadou, T.; Psomiadou, V.; Bagkavou, G. G.; Stathakis, C. I. Syntheses of ent-Aquilanol A and ent-Aquilanol B via Retro-Cycloisomerization of (-)-Caryophyllene Oxide. Access to Medium-Sized Oxygenated Carbocyclic Scaffolds. *Org. Lett.* **2022**, *24* (34), 6242−6246.

(13) (a) Sharma, J. N.; Al-Omran, A.; Parvathy, S. S. Role of nitric oxide in inflammatory diseases. *Inflammopharmacology* **2007**, *15* (6), 252−259. (b) Boje, K. M. Nitric oxide neurotoxicity in neurodegenerative diseases. *Front. Biosci.* **2004**, *9* (1−3), 763−776.

(14) (a) Combs, C. K.; Karlo, J. C.; Kao, S. C.; Landreth, G. E. β-Amyloid Stimulation of Microglia and Monocytes Results in TNFα-Dependent Expression of Inducible Nitric Oxide Synthase and Neuronal Apoptosis. *J. Neurosci.* **2001**, *21* (4), 1179−1188. (b) Takeuchi, H.; Jin, S.; Wang, J.; Zhang, G.; Kawanokuchi, J.; Kuno, R.; Sonobe, Y.; Mizuno, T.; Suzumura, A. Tumor Necrosis Factor-α Induces Neurotoxicity via Glutamate Release from Hemichannels of Activated Microglia in an Autocrine Manner. *J. Biol. Chem.* **2006**, *281* (30), 21362−21368.

(15) (a) Joosten, L. A. B.; Abdollahi-Roodsaz, S.; Dinarello, C. A.; O'Neill, L.; Netea, M. G. Toll-like receptors and chronic inflammation in rheumatic diseases: new developments. *Nat. Rev. Rheumatol.* **2016**, *12* (6), 344−357. (b) Sabroe, I.; Parker, L.; Dower, S.; Whyte, M. The role of TLR activation in inflammation. *J. Pathol.* **2008**, *214* (2), 126−135.

(16) (a) Drexler, S. K.; Foxwell, B. M. The role of Toll-like receptors in chronic inflammation. *Int. J. Biochem. Cell Biol.* **2010**, *42* (4), 506−518. (b) Kang, J. H.; Yang, H. W.; Park, J. H.; Shin, J. M.; Kim, T. H.; Lee, S. H.; Lee, H. M.; Park, I. H. Lipopolysaccharide regulates thymic stromal lymphopoietin expression via TLR4/MAPK/Akt/NF-κB-signaling pathways in nasal fibroblasts: differential inhibitory effects of macrolide and corticosteroid. *Int. Forum Allergy Rhinol.* **2021**, *11* (2), 144−152.

(17) Waetzig, V.; Czeloth, K.; Hidding, U.; Mielke, K.; Kanzow, M.; Brecht, S.; Goetz, M.; Lucius, R.; Herdegen, T.; Hanisch, U.-K. c-Jun N-terminal kinases (JNKs) mediate pro-inflammatory actions of microglia. *Glia* **2005**, *50* (3), 235−246.

(18) Chan, E. D.; Riches, D. W. IFN-γ + LPS induction of iNOS is modulated by ERK, JNK/SAPK, and p38^{<i>mapk</i>}in a mouse macrophage cell line. *Am. J. Physiol.: Cell Physiol.* **2001**, *280* (3), 441−450.

(19) Zhao, D.; Zhang, L. J.; Huang, T. Q.; Kim, J.; Gu, M.-Y.; Yang, H. O. Narciclasine inhibits LPS-induced neuroinflammation by modulating the Akt/IKK/NF-κB and JNK signaling pathways. *Phytomedicine* **2021**, *85*, 153540.

(20) Lyons, A.; Lynch, A. M.; Downer, E. J.; Hanley, R.; O'Sullivan, J. B.; Smith, A.; Lynch, M. A. Fractalkine-induced activation of the phosphatidylinositol-3 kinase pathway attentuates microglial activation in vivo and in vitro. *J. Neurochem.* **2009**, *110* (5), 1547−1556.

(21) Ohsawa, K.; Imai, Y.; Kanazawa, H.; Sasaki, Y.; Kohsaka, S. Involvement of Iba1 in membrane ruffling and phagocytosis of macrophages/microglia. *J. Cell Sci.* **2000**, *113*, 3073−3084.

(22) Dolomanov, O. V.; Bourhis, L. J.; Gildea, R. J.; Howard, J. A. K.; Puschmann, H. OLEX2: a complete structure solution, refinement and analysis program. *J. Appl. Crystallogr.* **2009**, *42* (2), 339−341.

(23) Sheldrick, G. SHELXT - Integrated space-group and crystal-structure determination. *Acta Crystallogr., Sect. A* **2015**, *71* (1), 3−8.

(24) Sheldrick, G. Crystal structure refinement with SHELXL. *Acta Crystallogr., Sect. C: Struct. Chem.* **2015**, *71* (1), 3−8.

https://doi.org/10.1021/acsomega.3c05783
ACS Omega 2023, 8, 43873−43882